Local structures of nanocrystalline GaN studied by XAFS

Zhongrui Li[a], Shiqiang Wei[a], Ying Wang[a], Xinyi Zhang[a], Kunquan Lu[b], and Xiaolong Chen[b]

[a]National Synchrotron Radiation Laboratory, University of Science & Technology of China, Hefei, 230029. P.R.China, [b]Institute of Phys., Chinese Academy of Sciences, Beijing, 100080. P. R. China.
E-mail: sqwei@ustc.edu.cn

X-ray absorption fine structure (XAFS) was used to investigate the local structures around Ga atoms in the hexagonal nanocrystalline and crystalline GaN under 78 and 300 K. For the first nearest neighbor coordination shell of Ga-N, the average bond length R (0.194 nm), coordination number N (4.0), thermal disorder σ_T (0.0052 nm) and static disorder σ_S (0.0007 nm) are nearly independent of the measured temperature and crystalline state. This indicates that the Ga-N covalent bond is much stronger, and the 4 nitrogen atoms in first nearest neighbor around Ga atoms keep the tetrahedral structure (Td). For the second nearest neighbor coordination shell of Ga-Ga, their bond lengths are about 0.318 nm. However, the σ_S (0.0057 nm) of nanocrystalline GaN is 0.0047 nm larger than that of crystalline GaN (0.001nm), and the σ_T of nanocrystalline is 0.0053 nm and 0.0085 nm at the temperature of 78 and 300 K, respectively. The result indicates that the difference of local structure around Ga atoms between nanocrystalline and crystalline GaN occurs mainly at the Ga-Ga second nearest-neighbor coordination shell. The reason is explained as the local lattice distortion and unsaturated surface atoms existing in nanocrystalline GaN.

Keywords: XAFS; GaN; local structure

1. Introduction

GaN-based semiconductors have been recognized as potential materials for the applications in fabricating blue vertical cavity surface-emitting lasers, high-brightness blue light emitting diodes, visible-blind detectors, high-temperature and high-power transistors, owing to their advantages of wide direct band gaps, high external luminescence quantum efficiencies, high break-down fields and excellent chemical stability (Someya, *et al.*, 1999; Nakamura, *et al.* 1997; Shur, *et al.*, 1997; Yoshida *et al.*, 1999). More recently, a lots of efforts have been paid on the studies of nanocrystalline GaN powder and GaN nano-rods for the usages in both mesoscopic research and future development of nano-devices (Chen *et al.*, 2000; Jegier *et al.*, 2000; Yang *et al.*, 2000), because of the size related effect of nanometer GaN.

However, GaN is characterized from high concentrations of point defects such as vacancies, nitrogen antisites and intersititials (Neugebauer *et al.*, 1994) as well as extended defects, *i.e.* dislocations and stacking faults, which have detrimental effects on the performance of lasers. Katsikini *et al.* (1998; 1999) have reported that the microstructures around the N and Ga atoms are distorted for the GaN thin films with XAFS technique. So far, there are few studies on the local structure of nanocrystalline GaN. It is not clearly enough for the size-tunable optical and electrical properties of nanocrystalline GaN (Alivisatos *et al.*, 1996). In order to improve the performance of GaN-based semiconductor device, it is necessary to investigate the local structures of GaN in detail. In the present work, the microstructures of nanocrystalline and crystal GaN at low and room temperature were determined using XAFS measurements at the Ga K-edge.

2. Experimental

Nanocrystalline GaN samples were obtained directly from reaction of metal Ga (99.999%), NH_4Cl (99.9%) and liquid ammonia in a platinum-linear stainless-steel autoclave at 623 K and 2000 atm for 120 h (Chen *et al.*, 2000). No impurity phase is detected under the resolution of Philips MPD diffractmeter (Cu Kα radiation). The average grain size according to the Scherrer formula is 11.8 nm. A transmission electron microscopy (TEM) image reveals that the fragment consists of nanocrystallines with grain sizes ranging from 5 to 25 nm, with an average size of 12 nm (Chen *et al.*, 2000). Crystalline GaN samples was obtained directly from reaction of metal Ga (99.999%) and high pure NH_3 (about 12 ml/min) in a pure-quartz reaction boat at 1300±10 K for 4 h (Chen *et al.*, 1999).

The Ga K-edge XAFS spectra for nanocrystalline and crystal GaN were measured on the U7C beam-line of Hefei National Synchrotron Radiation Laboratory (NSRL). The storage ring of NSRL was operated at 0.8 GeV with a maximum current of 160 mA, and the hard x-ray beam from a three-pole superconducting wiggler with a magnetic field intensity of 6 Tesla was used. The fixed-exit Si(111) flat double crystals were used as a monochromator. The XAFS data were collected in transmission mode with ionization chambers filled with flow of the mixed gases of N_2 and Ar at the temperature of 78 and 300 K, by using Keithley Model 6517 Electrometer to collect the electron charge directly. XAFS Data were analyzed by USTCXAFS1 software package compiled by Wan and Wei according to the standard procedures (Wan *et al.*, 1999; Sayers *et al.*, 1988) and UWXAFS3.0 software package (Stern *et al.*, 1995). The backscattering amplitude and phase shift functions were obtained using the model hexagonal GaN (a=0.318 nm, c=0.5168 nm) constructed with the program FEFF7 (Rehr, *et al.*, 1992).

3. Results and Discussion

The Ga K-edge adsorption spectra of nanocrystalline and crystal GaN were demonstrated in Figure 1 (μx *vs.* E). In the first 300 eV range above the Ga adsorption edge, there are eight strong oscillation peaks for crystalline GaN. The Ga edge adsorption spectra of nanocrystalline GaN have the similar shape as that of crystalline GaN, but a little weaker in amplitude, especially in the high-energy range. As compared with XAFS signals of GaN samples measured at lower temperature, the oscillation amplitudes of both nanocrystalline and crystalline GaN shrink dramatically at room temperature, which suggests that, the disorder of the coordinated atoms around Ga atom in GaN at 300K is higher than that at 78 K.

The EXAFS oscillation function $\chi(k)$ of GaN sample was obtained from the curves shown in Figure 1, by removing background, μ_0 fitting and transformation from energy to wave vector. The detailed data analyses have been shown elsewhere (Wei *et al.*, 1997; 2000). The EXAFS functions of $k^3\chi(k)$ are illustrated in Figure 2 for nanocrystalline and crystalline GaN. It clearly demonstrates that the oscillation magnitude of

 © 2001 International Union of Crystallography • Printed in Great Britain – all rights reserved

nanocrystalline GaN is much smaller than that of crystal GaN. This result further reveals that there is difference in the local structure around Ga atom between nanocrystalline GaN and crystalline GaN.

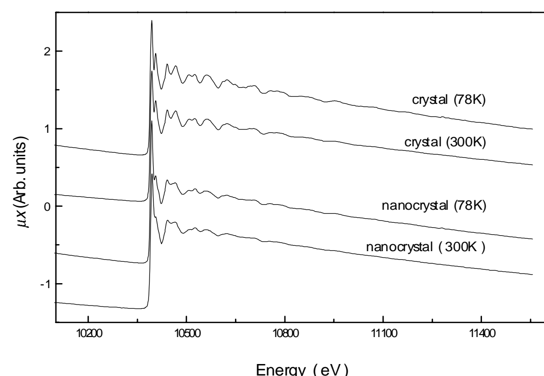

Figure 1
Ga *K*-edge absorption spectra for GaN samples

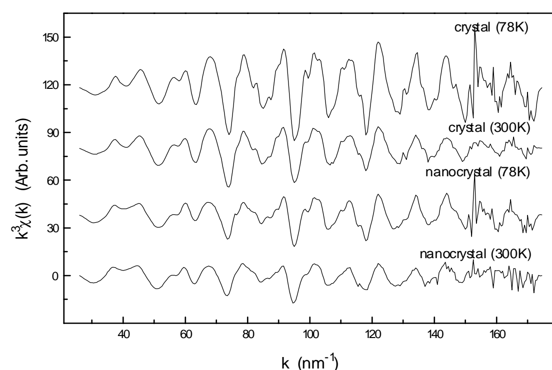

Figure 2
EXAFS oscillation functions $k^3\chi(k)$ *vs k* for GaN samples

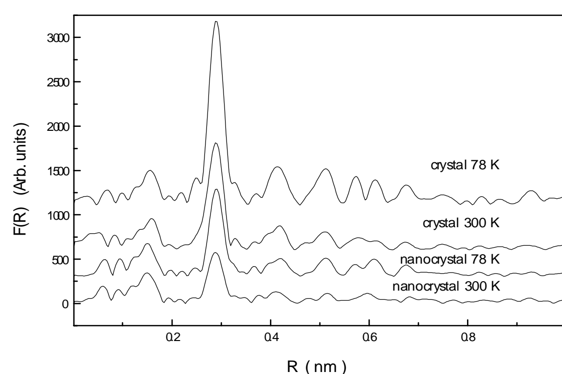

Figure 3
Radial distribution functions of GaN samples

Figure 3 displays the radial distribution functions (RDF) of GaN samples, which were obtained from Fourier transformation of their $k^3\chi(k)$. There are two strong coordination peaks located at 0.16 nm and 0.29 nm, corresponding to the first and second nearest neighbor coordination shells of Ga-N and Ga-Ga, respectively. Moreover, many peaks in the region of 0.4~0.7 nm, which is due to higher coordination shells. For the two samples measured at different temperature, the intensity of the first nearest Ga-N coordination shell are similar while the intensity of the second nearest Ga-Ga coordination shell strongly depends on the temperature and crystal status. The intensities of Ga-Ga coordination shell are 576, 987, 1210, 2071 for nanocrystalline GaN (300 K), GaN (78 K), crystalline GaN (300 K) and GaN (78 K), respectively. This result suggests that the RDF intensity of nanocrystalline GaN is about 50% as high as that of crystalline GaN. It exhibits that the local neighbor environment of Ga atom in nanocrystalline GaN sample is quite different from that of crystalline GaN.

In order to improve the precision for fitting the structural parameters around Ga atom in GaN sample, the peaks of Ga-N and Ga-Ga shells were isolated by a window function, and then an EXAFS oscillation signal of single shell was obtained by inverse Fourier transformation. The Debye-waller factor was separated into static disorder σ_S and thermal disorder σ_t for the benefit of considering the temperature effect on the disorder. Coordination distribution function g(R) was assumed as the convolution of Gaussian function P_G and exponential function P_E (Wu *et al.*, 1997; Wei *et al.*, 2000).

$$\begin{aligned} g(R) &= P_G \times P_E \\ P_E &= (1/2\sigma_S)(R-R_0)^2\exp[-(R-R_0)/\sigma_S], \quad R \geq R_0 \\ &= 0, \quad R < R_0 \end{aligned} \quad (1)$$

where R_0 is the distance of central atom to the close packing atom, the average distance at $R_0+\sigma_S$, EXAFS oscillation function should be expressed as

$$\chi(\kappa) = \frac{N_j F(\kappa) S_0^2(\kappa)}{kR^2\sqrt{1+4k^2\sigma_s^2}} \times \exp\left(-2\sigma_T^2 k^2\right) \times \exp\left(-\frac{2R}{\lambda(\kappa)}\right) \times \sin\left[2kR + \delta(\kappa) + \arctan(2k\sigma_s)\right], \quad (2)$$

where N_j is the number of atoms in the *j*th shell, k is the wave vector of photoelectron, F(k) is the magnitude of the backscattering amplitude of the *j*th-shell atoms, $S_0^2(k)$ is about 0.7 to 0.9 and is caused by many-body effects and dynamic relaxation (it is usually used together with $F_j(k)$ in data fitting), $\lambda(k)$, the mean free path of electron, $\delta(k)$ is the phase shift function.

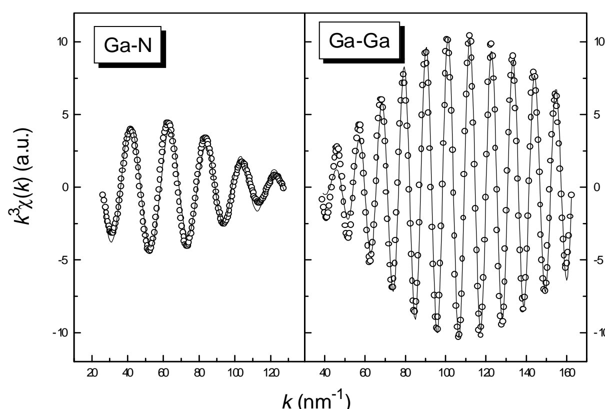

Figure 4
Comparison of inverse transformation of experimental spectra (open circle) and the fitting curves (solid line) for nanocrystalline GaN (78K)

Using the equation (2), F(k) and $\delta(k)$ function from FEFF7 (Rehr, *et al.*, 1992) for fitting the structural parameters of GaN

samples, the experimental data are well fitted with the theoretical curves as shown in Figure 4. The fitting results were listed in Table 1. The errors for the fitted parameters corrected as described by Stern *et al.* (1995) are estimated to be ±0.5 in coordination number N, ±0.002 nm in distance R, ±0.0005 nm in disorder factor σ.

Table 1
Structure parameters obtained from XAFS data of GaN samples

Sample	Pair	R / nm	N	σ_T / nm	σ_S / nm
Crystal,78K	Ga-N	0.194	4.0	0.0047	0.0005
	Ga-Ga	0.318	12.0	0.0051	0.0008
Crystal,300K	Ga-N	0.194	4.1	0.0050	0.0005
	Ga-Ga	0.318	12.1	0.0080	0.0010
Nanocrystal,78K	Ga-N	0.194	4.2	0.0051	0.0007
	Ga-Ga	0.318	10.5	0.0053	0.0055
Nanocrystal,300K	Ga-N	0.193	4.3	0.0052	0.0007
	Ga-Ga	0.319	10.3	0.0085	0.0057

Error bars of R_j, R_0, σ_T, σ_S and N are ±0.002 nm, ±0.002 nm, ±0.0005 nm, ±0.0005 nm and ±0.5, respectively.

GaN exists in two types, the cubic (zincblende) and the hexagonal (wurtzite). X-ray powder diffraction result indicates all samples in this work are hexagonal GaN. Crystalline GaN belongs to space group of P63mc (Wells *et al*., 1975). The first and second nearest neighbors of Ga atom are 4 N atoms at 0.194 nm and 12 Ga atoms at 0.318 nm. Seen from Figure 3 and Table 1, it can be found that the peak position and intensity of Ga-N coordination shell are almost the same for crystalline and nanocrystalline GaN samples. The bond length and coordination number are 0.194 nm and 4, which are identical with those of standard hexagonal GaN crystal. Moreover, the σ_T and σ_S of Ga-N coordination shell are nearly independent of temperature and crystalline state. The results imply that the Ga-N covalent bond is much stronger, and the first nearest neighbor geometry is tetrahetral structure T_d. However, the structural difference between nanocrystalline and crystal GaN occurs in the second nearest Ga-Ga coordination shell. Although the Ga-Ga magnitude peaks shown in figure 3 keep at the same position, the intensity of Ga-Ga coordination shell decreases by half while the measured temperature is from 78 to 298 K or the state is from the crystalline to the nanocrystalline. The structural parameters in the Table 1 indicate that the σ_T of the second nearest Ga-Ga coordination shell is 0.0051 nm at 78 K and 0.0080 nm at 300 K for crystalline GaN. Our results are in good agreement with Katsikini *et al.'s* (1999) results that reported that the disorder of the second nearest Ga-Ga coordination shell is 0.0052 nm and 0.0073 nm at 100 and 290 K, respectivly. In addition, there is nearly the same value for the σ_T of Ga-Ga shell between of nanocrystalline and crystalline GaN, their difference are below 0.0005 nm. Nevertheless, the static disorder σ_s (0.0055 nm) in the second nearest Ga-Ga shell of nanocrystalline GaN (78 K) is 0.0047 nm larger than that (0.0008 nm) of crystalline GaN (78 K). This reveals that there are local lattice distortions in nanocrystalline GaN.

4. Conclusions

The XAFS results indicated that the local structure difference between nanocrystalline and crystalline GaN samples, mainly occurs in the second nearest Ga-Ga neighbor shell. The σ_S (0.0055 nm) of Ga-Ga shell of nanocrystalline GaN (78 K) is 0.0047 nm larger than that (0.0008 nm) of crystalline GaN (78 K). We consider that the reason is local structure distortions and unsaturated surface atoms in nanocrystalline GaN. The Ga-N covalent bond in GaN samples is much stronger, whose thermal disorder σ_T and static disorder σ_S are nearly independent of the measured temperature and crystalline state. The interaction force in the second nearest Ga-Ga neighbor coordination shell is relatively weaker, and temperature and crystalline state can strongly influence their σ_T and σ_S.

Acknowledgements

We would like to thank National Synchrotron Radiation Laboratory and Beijing Synchrotron Radiation Facility for giving us the beam time for XAFS measurement. This work was supported by "100 people plan" and "9•5 programs" of Chinese Academy of Sciences and National Natural Science Foundation of China.

References

Alivisatos, A. P., (1996). *Science* **271**, 933-937.

Chen, X.L., Cao, Y.G., Lan, Y.C., Xu, X. P., Li, J.Q., Lu, K.Q., Jiang, P.Z., Bai, Z.G., Yu,Y.D. & Liang, J.K., (2000). *J. Crystal. Growth*. **209**(1), 208-212.

Chen, X. L., Lan, Y.C, Liang, J. K., Cheng, X.R., Xu, Y.P., Xu, T., Jiang, P.Z., & Lu, K.Q., (1999), *Chin. Phys. Lett.*,**16**(2): 107-108.

Katsikini, M., Rossner, H., Fieber-Erdmann, M., Holub-Krappe, E., Moustakas, T. D., & Paloura, E.C., (1999). *J Synchrotron Rad.* **6**, 561-563.

Nakamura, S., (1997). *Meter. Res. Bull.* **22**(2), 29-35.

Neugebauer, J., & Van de Walle, C., (1994). *Phys. Rev. B* **50**, 8067-8071.

Sayers, D. E., & Bunker, B. A., (1988). *X-ray Absorption, Principles, Applications, Techniques of EXAFS, SEXAFS and XANES,* P.211, edited by Koningsberger, D.C., and Prins, R., John Wiley and Sons, Inc.

Shur, M. S. & Khan, M. A., (1997). *Mater. Res. Bull.* **22**(2): 44-48.

Someya, T., Werner, R., Forchel, A., Catalano, M., Cingolani, R., and Arakawa, Y., (1999). *Science*, **285**, 1905-1906.

Stern, E., Newville, M., Ravel, B., Yacoby, Y., & Haskel, D., *Physica B.* 208/209 (1995) 117.

Rehr, J.J., Zabinsky, S.I., & Albers, R.C., (1992).*Phys. Rev. Lett.* **69**, 3397-3400

Wan, X. H. & Wei, S.Q., *USTCXAFS Software Package* (May, 1999).

Wei, S.Q., Oyanagi, H., Kawanami, H., Sakamoto, K., Sakamto, T. , Tamura, K. , Saini, N.L. & Uosaki, K. , (1997).*J.Appl.Phys.* **82**, 4810-4815.

Wei, S.Q., Oyanagi, H., Sakamoto, K., Tamura, K., & Pearsall, T.P., (2000). *Phys.Rev. B* **62**, 1883-1888.

Wei, S.Q., Oyanagi, H., Liu, W.H., Hu, T.D., S.L. Yin, & Bian, G.Z., (2000). *J. Non-crystalline solids*, **275**, 160-168.

Wells F. W., (1975). *Structural Inorganic Chemistry,* P1012, Oxford University Press.

Wu L.W., Wei S.Q., Wang, B. & Liu, W.H., (1997). *J. Phys. CM.*, **9**, 3521-3128.

Yoshida, S. & Susuki, J., (1999). *J. Appl. Phys.* **85**, 7931-7936.

 Received 31 July 2000 • Accepted 20 December 2000